

# CAAP Quarterly Report

Date of Report: October 10<sup>th</sup> 2019

Prepared for: *U.S. DOT Pipeline and Hazardous Materials Safety Administration*

Contract Number: 693JK31850008CAAP

Project Title: Fluorescent Chemical Sensor Array for Detecting and Locating Pipeline Internal Corrosive Environment

Prepared by: Dr. Ying Huang, Dr. Wenfang Sun, and Dr. Hao Wang

Contact Information: Dr. Ying Huang, Email: ying.huang@ndsu.edu, Phone: 701.231.7651

For quarterly period ending: October 10<sup>th</sup> 2019

## **Business and Activity Section**

### **(a) Contract Activity**

Discussion about contract modifications or proposed modifications

None.

Discussion about materials purchased

None.

### **(b) Status Update of Past Quarter Activities**

In this quarter, the university research team performed the planned activities in last quarter and worked on Task 2.1 and Task 2.2 of the above-mentioned project, including 1) writing the sensors into PMMA and epoxy resin to test the feasibility and optimize the matrix materials with two materials were tested, and PMMA with sensors was tested to be sensitive to Fe<sup>2+</sup> but not the other ions and epoxy with sensors was tested to be insensitive to any ions [Task 2.1], 2) setting up CFD simulation model and starting to simulate the pipeline environment for survivability study [Task 2.2], and 3) conducting experiments on optimizing sensor design and survivability with different thicknesses under pigging activities and corresponding finite element simulation as verification [Task 2.2].

### **(c) Cost share activity**

Tuition Waiver for two graduate students with \$9,364 of cost share in this quarter.

## **(d) Task 2: Development of Fluorescent/Colorimetric Chemical Sensor Array for Internal Corrosive Water Detection**

Two subtasks were worked on during this quarter including Task 2.1 (Development of Fluorescent/Colorimetric Chemical Sensor Array) and Task 2.2 (Calibration of the Fluorescent/colorimetric Chemical Sensor Array). The detail findings are described as below:

### **1. Background and Objectives in the 4<sup>th</sup> Quarter**

#### ***1.1 Background***

This project is designed to develop passive colorimetric/fluorescent chemical sensor array for locating and detecting corrosive water inside pipes. Inside the pipelines, the transported crude oil may include a hot mixture of free water, carbon dioxide (CO<sub>2</sub>), hydrogen sulfide (H<sub>2</sub>S) and microorganisms. The different chemical components inside oil/water environment such as HCO<sub>3</sub><sup>-</sup> / CO<sub>3</sub><sup>2-</sup>, Fe<sup>3+</sup>, S<sup>2-</sup>, H<sup>+</sup> or pH may result in different internal corrosion mechanisms, such as sweet corrosion or sour corrosion. The passive colorimetric sensor array to be developed in this project is intended to detect the concentration changes of the five above mentioned important chemical species in the internal oil/water environment of the pipeline and use these detected environmental data to predict the internal corrosion progressing of pipelines.

#### ***1.2 Objectives in the 4<sup>th</sup> Quarter***

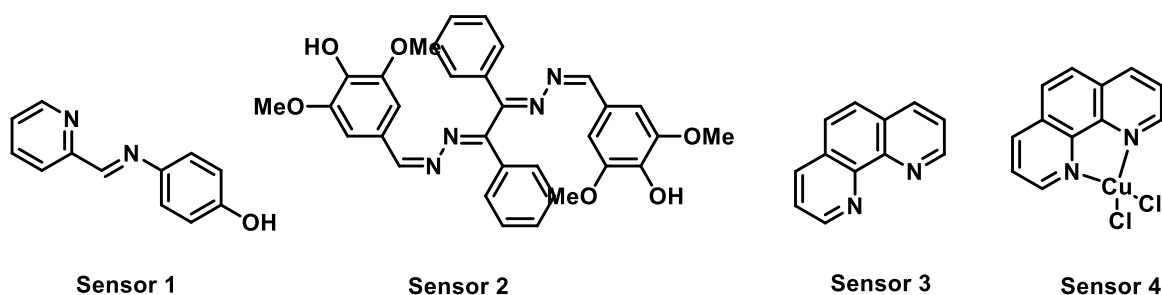
In this quarter, we will write the sensor into two different polymeric matrix to find the material which could work to host the sensor (the two polymeric matrix tested in this quarter include PMMA and epoxy), set up the CFD model of the pipeline which will have sensors to be attached for survivability analysis in water/oil environment, conduct lab experiments to test the survivability of the sensor under pigging service (cleaning) and optimize the sensor's thickness based on the pigging service, and based on the test results, update the finite element model analysis for future sensor design needs.

### **2. Results and Discussions**

#### ***2.1 Development of Fluorescent/Colorimetric Chemical Sensor Array (Task 2.1)***

In this quarter, we wrote the sensor into two different the commercially available polymeric matrix, PMMA and epoxy. The sensing ability of the sensing molecules as shown in Table 1 for each of the sensor molecules that we synthesized and reported in Quarterly Report 2 were incorporated into the two polymeric matrix, PMMA and epoxy resin films, and their sensing abilities toward S<sup>2-</sup>, Fe<sup>3+</sup>, HCO<sub>3</sub><sup>-</sup> / CO<sub>3</sub><sup>2-</sup>, were tested respectively. Experimental results showed that the sensor can be successfully wrote into the PMMA for sensing Fe<sup>2+</sup> but not the other ions (HCO<sub>3</sub><sup>-</sup> / CO<sub>3</sub><sup>2-</sup>, S<sup>2-</sup>, Fe<sup>3+</sup>) and epoxy with sensors was tested to be insensitive to any ions. So we will use PMMA to host the Fe<sup>2+</sup> sensor in future testing of survivability. In next quarter, we will focus on testing other porous polymer matrix to dope our sensor molecules to find an appropriate host matrix for other ions (CO<sub>3</sub><sup>2-</sup>, S<sup>2-</sup>, Fe<sup>3+</sup>).

**Table 1.** Different sensors to be written in the PMMA and epoxy films



**2.1.1 Phenanthroline (Phen) sensing of Fe<sup>2+</sup> ion in solution and in PMMA films**

The commercial available compound, Phenanthroline (Phen) (Sensor 3 in Table 1), was used to sense for Fe<sup>2+</sup> cation in both solution and PMMA. As shown in Fig. 1, the color of dichloromethane (DCM) solution of phenanthroline was pale yellow, but the color changed to red upon addition of FeCl<sub>2</sub> aqueous solution. Such a drastic color change should be ascribed to the coordination of Phen with Fe<sup>2+</sup>, which induced the charge transfer transition in the formed complex. Such a drastic color change is transferred to the PMMA film doped with 10% of Phen. When drops of 5% FeCl<sub>2</sub> aqueous solution was put on the surface of the Phen/PMMA film, the color of the film surface changed to red immediately. Upon washing and being ultrasonicated in deionized water three times, the color of the PMMA film surface essentially recovered.

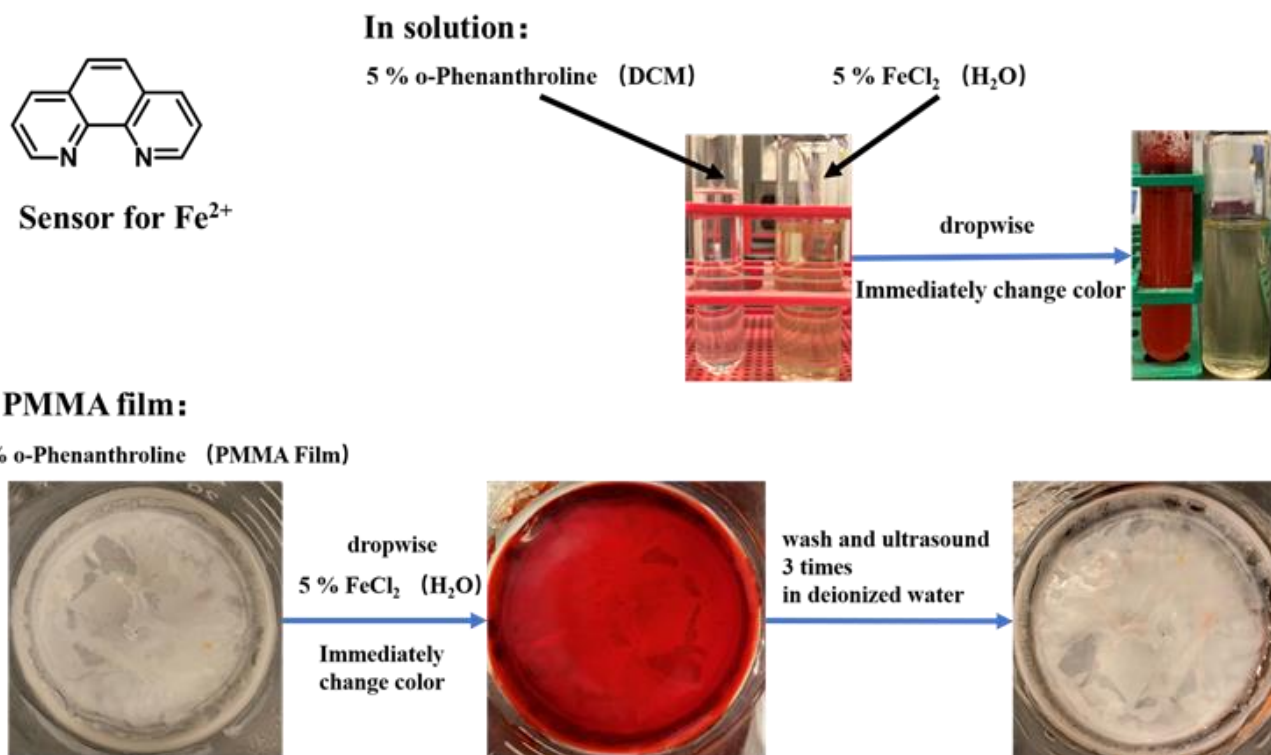


**Fig. 1.** Phenanthroline sensing toward FeCl<sub>2</sub> in solution and in PMMA film

Such a color change/decoloring cycle can be repeated multiple times, as demonstrated in Fig. 2. Phen was also doped into resin films to test if there is a similar color change upon exposure to Fe<sup>2+</sup> ion aqueous solution. As summarized in Table 2, no color change occurred in the resin films.

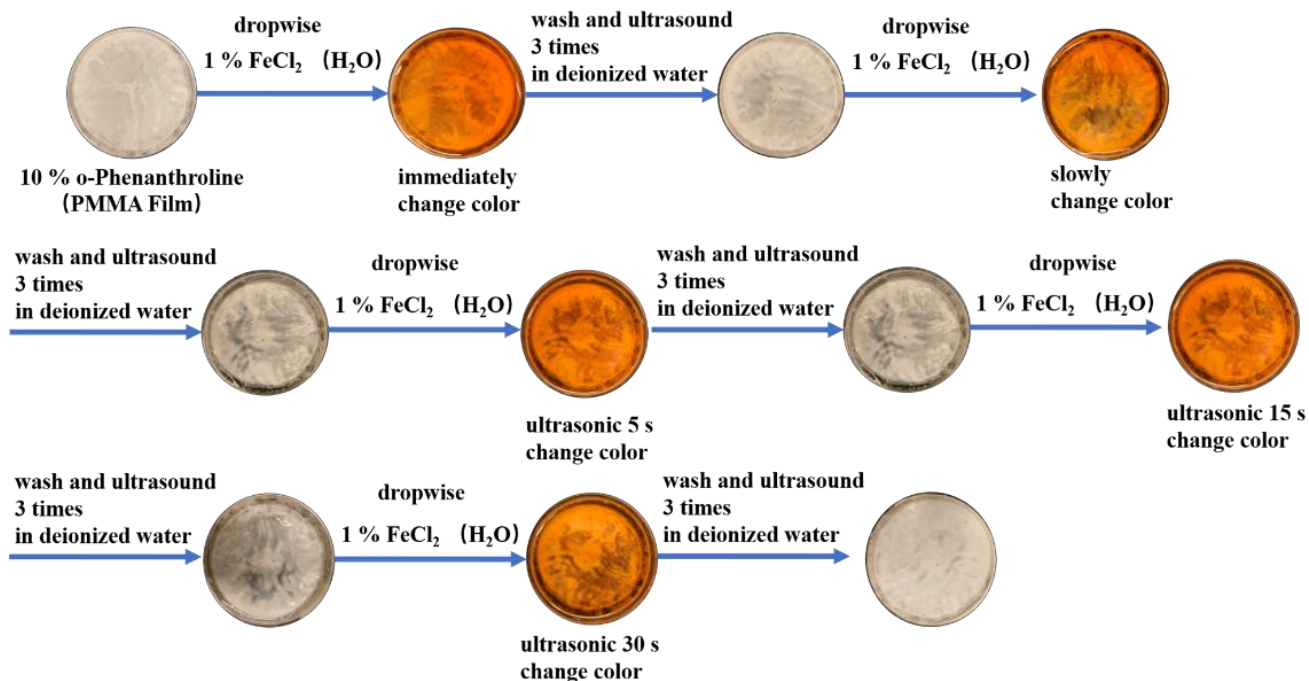


**Fig. 2.** Color/decolor cycle for Phen/PMMA film

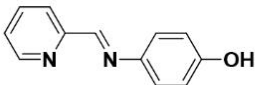
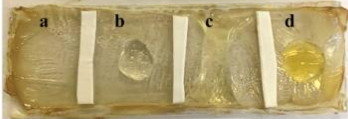
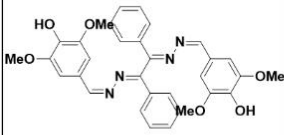
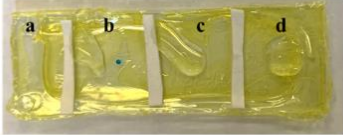
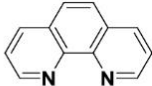
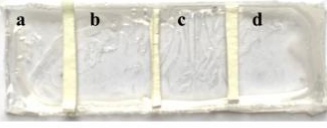
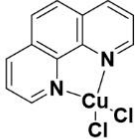
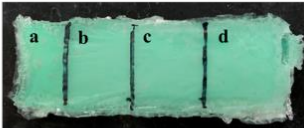
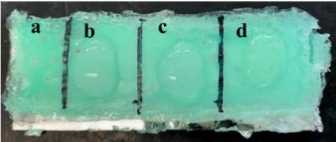
### 2.1.2 PhenCuCl<sub>2</sub> for S<sup>2-</sup>, Fe<sup>3+</sup>, and HCO<sub>3</sub><sup>-</sup> / CO<sub>3</sub><sup>2-</sup> sensing

Using Phen as the ligand, we synthesized the PhenCuCl<sub>2</sub> complex (Sensor 4 in Table 1, the color of the complex solution is jade) and intended to use it for S<sup>2-</sup> sensing. We doped this sensor into PMMA and epoxy resin films and tested the films' color response upon exposure to Na<sub>2</sub>S aqueous solution. Unfortunately, there was no color change in these films upon exposure to Na<sub>2</sub>S aqueous solution, regardless whether PMMA or resin was used as the matrix (see pictures in Tables 1 and 2, the fourth row).

In addition, we also prepared the PMMA and resin films doped with the Fe<sup>3+</sup> sensor (Sensor 1 in Table 1) and HCO<sub>3</sub><sup>-</sup> / CO<sub>3</sub><sup>2-</sup> sensor (Sensor 2 in Table 1) that we reported in the second quarter and tested their sensing responses toward Fe<sup>3+</sup> and HCO<sub>3</sub><sup>-</sup> / CO<sub>3</sub><sup>2-</sup> species. A drop of the analyte solution with different concentrations (0.1%, 1%, 5%) was added on the surface of the PMMA (as seen in Table 2) and epoxy resin films (as seen in Table 3) to observe the color changes. As summarized in Tables 2 and 3, except for Phen/PMMA film that showed a drastic color change upon exposure to Fe<sup>2+</sup>, all of the other films did not exhibit observable color change in these films regardless these sensor molecules exhibiting a very clear color change to analytes in solutions.

To test whether over-time exposure will induce color changes, the resin films were immersed in the corresponding ionic solutions with a concentration of 10%. As shown in Fig. 3, after 16-hour immersion in the analyte solutions, only slight responses were observed and no visible color changes from either PMMA or epoxy resin matrix were observed for the HCO<sub>3</sub><sup>-</sup> / CO<sub>3</sub><sup>2-</sup>, S<sup>2-</sup>, Fe<sup>3+</sup>. *Since the sensor is insensitive to these species, due to the similarity between the sensor for Fe<sup>3+</sup> and H<sup>+</sup>, it is expected that PMMA and epoxy resin matrix would not work for H<sup>+</sup> or pH value. So no test was performed on testing the H<sup>+</sup> or pH value. It will be tested when an appropriate polymer is selected.*

**Table 2.** Ion response of the PMMA films doped with different sensors

Sensor	Ion solution	Sensor@PMMA Film	ion solution+ Sensor@PMMA Film
	$\text{Fe}^{3+}$		 blank    0.1%    1%    5% ×        ×        ×
	$\text{CO}_3^{2-}$		 blank    0.1%    1%    5% ×        ×        ×
	$\text{Fe}^{2+}$		 blank    0.1%    1%    5% ×        √        √
	$\text{S}^{2-}$		 blank    0.1%    1%    5% ×        ×        ×

**Table 3.** Ion response of the epoxy resin films doped with different sensors

Sensor	Ion solution	Sensor@resin Film	Ion solution+ Sensor@resin Film 5 min	Ion solution+ Sensor@resin Film 30 min	Wash with water Sensor@resin Film
1	Fe <sup>3+</sup>		 blank 0.1% 1% 5%	 blank 0.1% 1% 5%	 × × ×
2	CO <sub>3</sub> <sup>2-</sup>		 blank 0.1% 1% 5%	 blank 0.1% 1% 5%	 × × ×
3	Fe <sup>2+</sup>		 blank 0.1% 1% 5%	 blank 0.1% 1% 5%	 × × ×
4	S <sup>2-</sup>		 blank 0.1% 1% 5%	 blank 0.1% 1% 5%	 × × ×

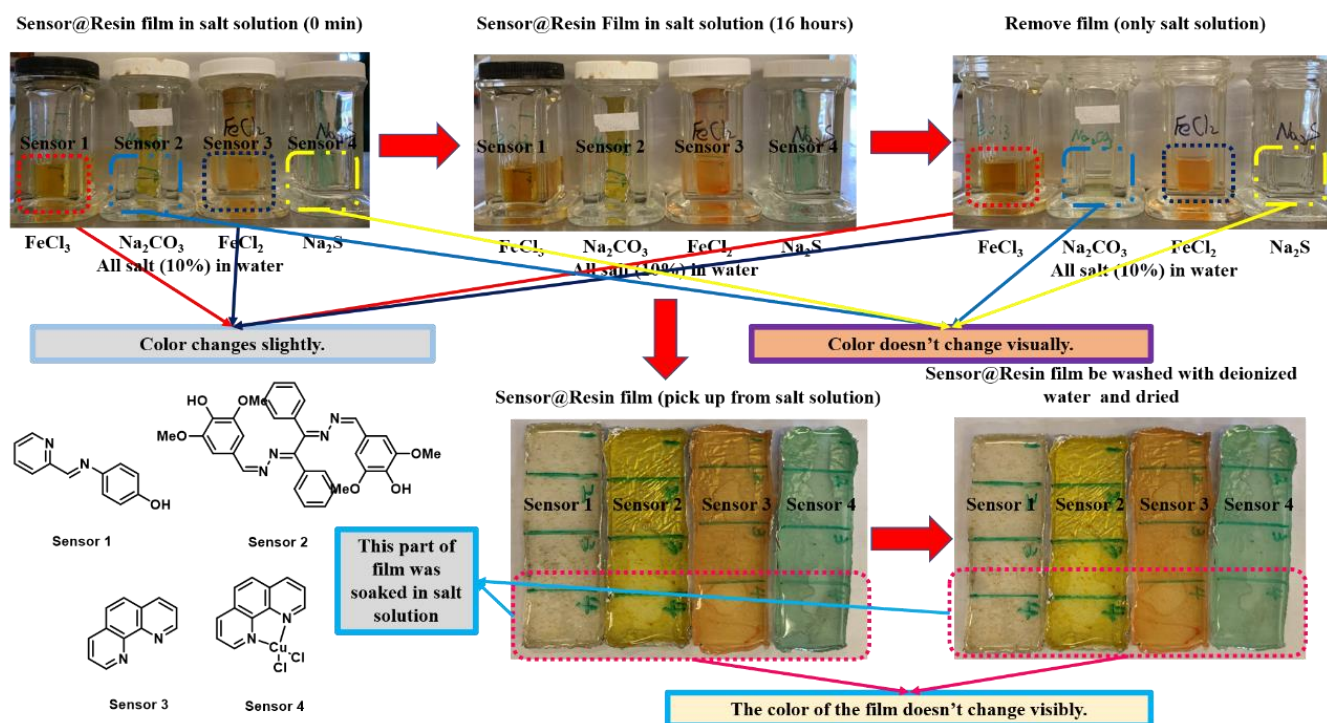


**Fig. 3.** Immersion of the resin films doped with sensor molecules to the analyte solutions for 16 hours.

The inactivity of the  $\text{HCO}_3^- / \text{CO}_3^{2-}$ ,  $\text{S}^{2-}$ ,  $\text{Fe}^{3+}$ ,  $\text{H}^+/\text{pH}$  sensor molecules in PMMA or epoxy resin polymer films probably is due to the fact that they are the dense films. The successful writing of  $\text{Fe}^{2+}$  sensor into the PMMA and the slight color changes of 16 hours doping in solutions showed confidence that if a polymer is porous enough or more permeable, the sensor can be written into the polymer. Thus, to allow the analyte molecules to penetrate through the films and interact with the sensor molecules, in the next quarter, we will focus on finding an appropriate porous or permeable polymer matrix to dope our  $\text{HCO}_3^- / \text{CO}_3^{2-}$ ,  $\text{S}^{2-}$ ,  $\text{Fe}^{3+}$  sensor molecules in order to capture the analytes. One of the polymer which will be tested include the poly(vinylidene fluoride) (PVDF), the polyethersulfone type polymer poly[2-(4-(diphenylsulfonyl)-phenoxy)-6-(4-phenoxy) pyridine](PDSPP), which have been successfully used as porous polymeric

membrane based on literatures. In addition, we will also seek other possible approaches such as permeable polymer films and attaching the films on epoxy with sufficient protection for possible sensor installation to ensure a possible workable sensor for the application.

## **2.2 Calibration of the Fluorescent/colorimetric Chemical Sensor Array (Task 2.2)**

Before widely deployed, survivability of sensor arrays is an essential issue for an expected service period. When the oil/gas products are being transported, sever heat, pressure and speed are applied to reach the demand for flow rate. All these destructive external conditions pose a huge challenge to the survivability of the sensors. In addition, the regular cleaning behavior by introducing Pipeline Investigation Gauges induces the most severe scraping impact on sensors which could lead to mechanical shedding failure. To this concern, experimental investigation and theoretical analysis of sensor survivability is one of the crucial subjects upon the utilizing. In this quarter, we have developed computational fluid dynamics (CFD) model and calculated the flow pattern of oil-water two phase flow in a horizontal straight pipeline. In addition, we also conducted experiments to test the sensor survivability under pigging service (cleaning), and optimize the sensor size (thickness) using the finite element and experimental analysis. In next quarter, the CFD model can be further developed to calculate flow patterns and wall shear stresses of flow in the pipeline with different oil concentrations and pipe geometries. The lab experiments will conform the survivability of the sensor in oil environments and whether cleaning services are needed. These results will be useful to analyze the internal corrosion potential of pipeline and the optimized design and placement of chemical sensors.

### **2.2.1 Sensor Array Survivability in Oil/Water Environment**

#### **2.2.1.1 CFD Model Setup**

The CFD model was developed using the Fluent software. The fluid flow in pipelines was oil-water two phase flow. The pipeline is horizontal straight with a diameter of 0.1m and a length of 1m. Mesh sensitivity analysis was conducted considering the balance between computation efficiency and accuracy. Three-dimension model contains 96,640 elements. Fig. 4 shows the mesh of 3-D model. The fluid flow was considered as transient, and the effect of temperature fluctuations on the fluid flow was negligible. The Canadian crude oil with density of 914 kg and viscosity 37.2 cSt at 40°C was used for simulation. The water/oil weight percentage was 40% water and 60% oil. For this analysis, the operating pressure was temporarily set as atmospheric pressure. In the future analysis, the operating pressure will be adjusted to a normal operation pressure of a practical pipeline.

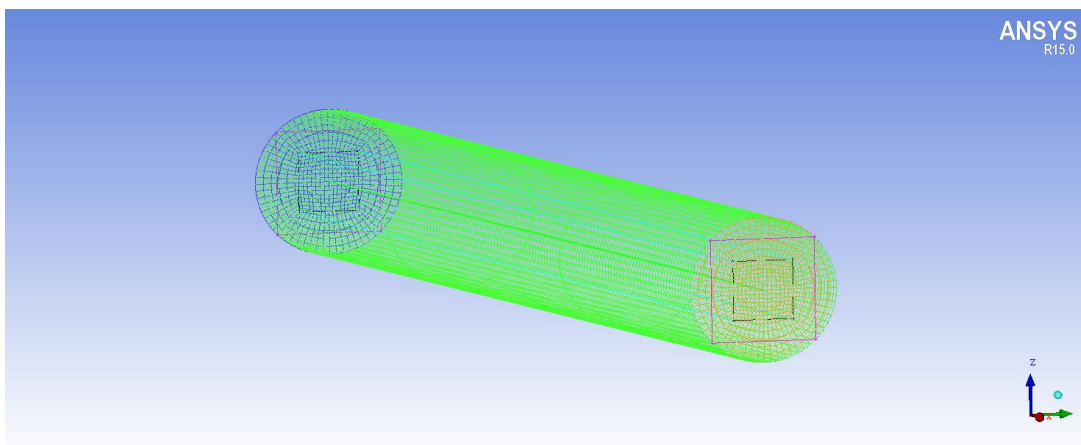


**Fig. 4.** Mesh of the 3-D CFD model

Since it is a two-phase simulation for water/oil flow, the volume of fraction (VOF) model was chosen. Phase changes were not considered with this model. The realizable k-epsilon model was used for turbulent fluid and standard wall functions were selected assuming that the fluid was stagnant at the wall of the pipe. According to the Reynolds equation as in Equation (1),

$$Re = \frac{VD}{\nu} \tag{1}$$

where,  $Re$  is Reynolds number,  $V$  is the velocity of fluid (m/s),  $D$  is diameter of the pipeline (m) and  $\nu$  is viscosity (m<sup>2</sup>/s), we can calculate the velocity of the laminar flow in the pipe as:

$$V = \frac{Re\nu}{D} = \frac{2300 \times (3.72 \times 10^{-5} \times 0.6 + 1.003 \times 10^{-6} \times 0.4)}{0.1} = 0.523 \text{ m/s}$$

This means when velocity is below 0.5 m/s, the fluid could be treated as laminar fluid and the fluid is treated as turbulence when the velocity is bigger than 0.5m/s. For the inlet of pipeline, the velocity inlet was applied as 0.1, 0.2, 0.3, 0.5, and 1 m/s respectively. For the outlet of the pipeline, the pressure outlet was used. The wall boundary condition was used to restrain the liquid. The simulation was time-dependent (transient) with 200 time steps. A time step was 0.05s and 40 iterations were used at each time step.

### 2.2.1.2 Preliminary Results of Flow Pattern

Fig. 5 shows the distribution of the volume fraction of oil in the fluid in the straight pipe at various flow velocities. The color bar indicates the volume percentage of oil in the fluid. The water phase, as indicated by blue color, tends to accumulate at the bottom of the pipe as the flow velocity is small. At the high flow velocity of 0.5 and 1m/s, oil-in-water and water-in-oil emulsions are formed. In next quarter, sensors with PMMA materials will be assumed to be placed in the bottom surface of the pipe with the high velocity flows to simulate the analysis of sensor survivability.

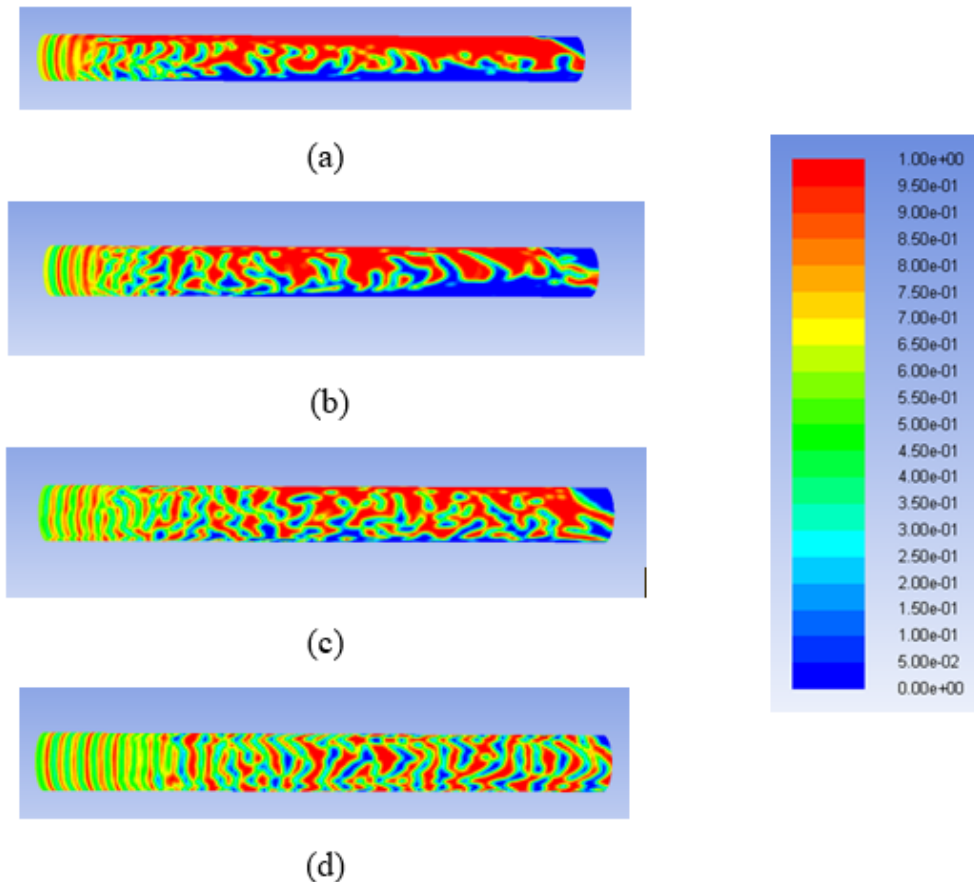


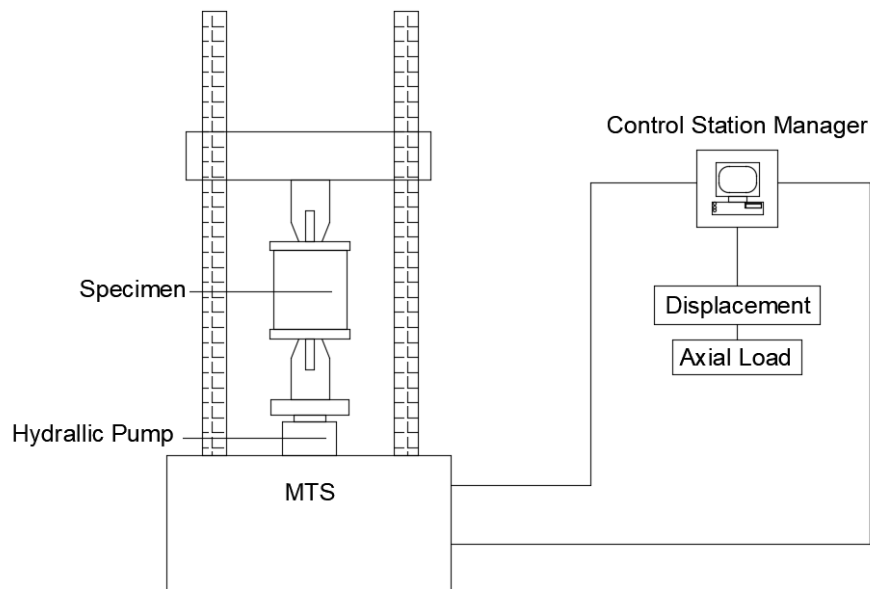
**Fig. 5.** Distribution of volume fraction of oil at various flow velocities (a) 0.2 m/s, (b) 0.3 m/s, (c) 0.5 m/s, (d) 1 m/s

### 2.2.2 Experimental Study of Sensor Survivability

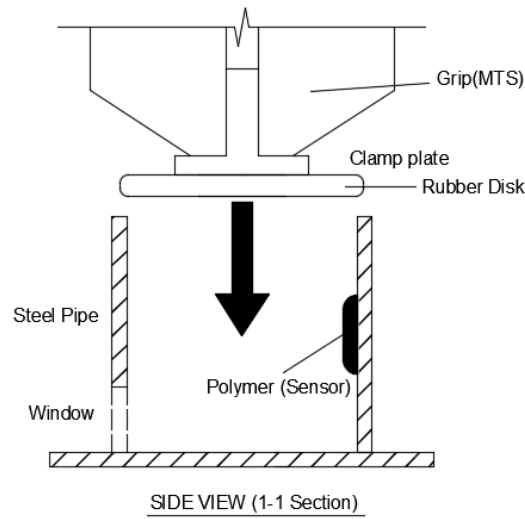
To experimentally test the survivability of the sensor array, in this quarter, we successfully designed a test procedure in laboratory to simulate and test the sensor performance when a PIG is passing the sensor. Based on the designed tests, experiments were performed on some possible example sensors under PIG activities. In addition, equivalent finite element model (FEM) simulation were updated based on the test to validate the test results. With the test and simulation results, we developed a preliminary analysis method to establish a reliable survivability model for the fluorescent sensors.

#### 2.2.2.1 Experimental Design

Pigging is now a standard procedure in petroleum and natural gas industry. Fluid or gas is pumped upstream to provide necessary force for cleaning the wax and sediments or dewatering. The traveling portion of a typical PIG is made up of a rigid and hollow center body and two sets of sealing disks. Clamp plates are used to hold each sealing disk in place on either side of the main rigid body. The PIG with sealing disks made of polyurethane rubber is usually propelled down the line due to the flow in the pipeline. In this research, according to the actual procedure of pigging service, a rubber disk made of polyurethane and steel pipes with 6'' and 8'' diameter were selected as test specimens to simulate the pigging process. In the experimental test, MTS hydraulic loading machine was used to drive the rubber disk through the pipeline, and the equipped data collection system could record the axial load and displacement of the lower loading Grip. So that the friction on the inner pipe walls, the sensor and whatever the force preventing the pigging motion would be recorded for further analysis. Fig. 6 shows the detail experiment design.



(a) Experimental setup



(b) Specimen design

**Fig. 6.** Experimental design

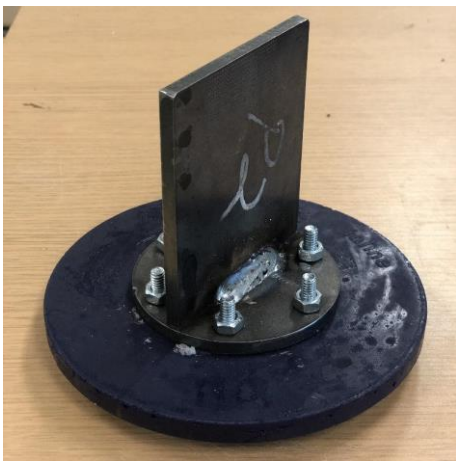
The tested specimens are categorized into two groups due to the different dimensions of the pipes and rubber plates, which is shown in Table 4.

**Table 4.** Details of specimen dimensions

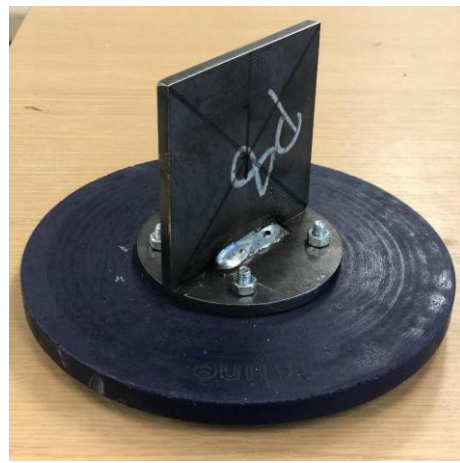
NSP	Pipe Type	Pipe Inner Diameter	Pipe Wall Thickness	Plate Diameter	Plate Thickness
6	6" Pipe	6.065"	0.280"	6.368"	0.375"
8	8" Pipe	7.981"	0.322"	8.380"	0.5"

2.2.2.2 Specimen Manufacturing and Test Setup

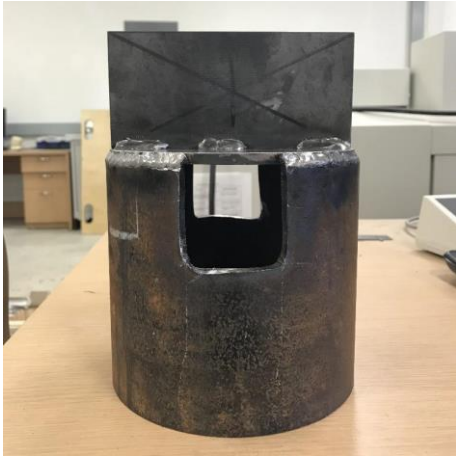
After the drafting of experiment sketch, specimens were manufactured in local steel companies to meet the test requirements. For the pipes, the 6 in. steel pipes covered with lid on one side were manufactured in Mid America Steel, which have two windows opened in each pipe on the covered ends. The purpose of the opening windows were to circulate the air when the rubber disks are going in and out of the pipes. Each pipe had a steel-plate handle with 1/4" thickness to guarantee the proper grip of the lower loading jig (MTS). For the rubber plates, standard 6" and 8" PIG attachment polyurethane disks were chosen as specimens. In addition, two pieces of circular plates were used to clamp the rubber plates in the middle, which using bolts and nuts to fix their locations. Also, same with the steel pipes, square-plate handles were used for the attachment of the upper loading jig. The details of the specimens are shown in Fig.7.



(a) 6" rubber disk



(b) 8" rubber disk



(c) 6" steel pipe



(d) 8" steel pipe

**Fig. 7. Specimen manufacturing**

To drive the disk smoothly, protect the rubber, and get stable experimental data, a displacement-control program were set to the hydraulic loading machine. The test parameters are shown in Table 5, in which Initial Displacement means the gap between the starting point and the contact point at the pipe is 5mm. The test setup is shown in Fig. 8.



**Fig. 8. Test setup**

**Table 5. Test Setup Parameters**

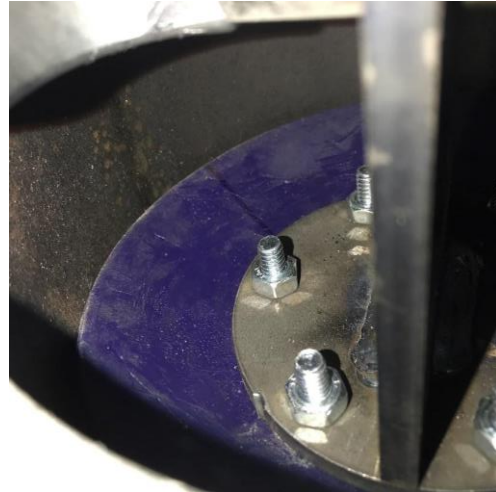
DISPLACEMENT RATE	DISPLACEMENT INCREMENT	DISPLACEMENT MODE	INITIAL DISPLACEMENT
0.3MM/S	101.6mm(4inches)	Monotonic	-5mm

### 2.2.2.3 Test Results

According to the preliminary observation of the test, the deformation of the rubber disk can be categorized into two stages. Stage 1 is the deformation outside the steel pipe (Fig. 9 (a)), in which the rubber disk deforms because of its oversized outer edge. After the certain point of the axial displacement that is the start point of Stage 2, the oversized disk is completely squeezed into the pipe, from where the stable slip motion would happen, and the axial load is to overcome the friction between the disk and the pipe (Fig. 9 (b)).



(a) Disk deformation stage 1



(b) Disk deformation stage 2

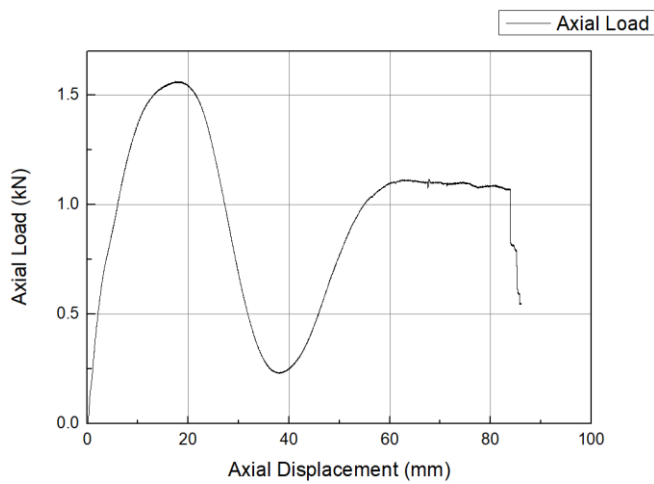
**Fig. 9.** Deformation of the disk

Given by the load sensors in loading Jigs of the MTS, the load-displacement curves could be drawn as in Fig. 10 for 6 inches and 8 inches diameter pipes with the rubber going from the top to the bottom of a pipe, respectively. It is shown from the curve that in the deformation stage 1, the axial load showed a fluctuation characteristic which reached a high value and then re-raise to a specific value and then entered the deformation stage 2. *In the stage 2, when the axial load remained stable, friction is only directly related to axial load as:*

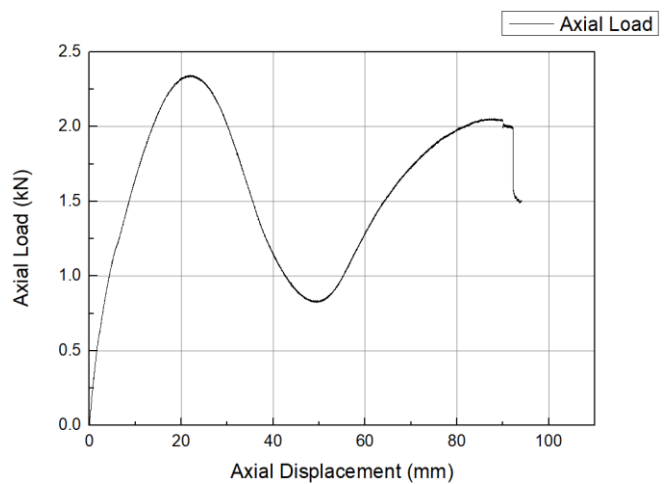
$$F_f = \mu \times P \quad (2)$$

*in which,  $F_f$  is friction force,  $\mu$ , is the friction coefficient of the material, and  $P$  is the axial load.*

*Since the friction coefficient,  $\mu$ , of the pipe or the polymer is known when the material is determined and not changing with the rubber pigging passing or not, from the recorded axial load, different friction on sensors in different thickness can be calculated for the shear force for a sensor to survive.*



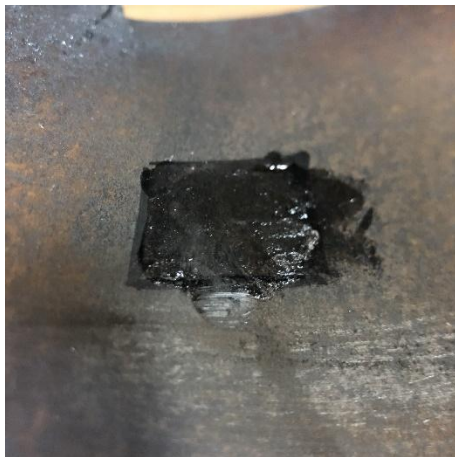
(a) Load-displacement curve of 6" pipe



(b) Load-displacement curve of 8" pipe

**Fig. 10.** Load-displacement curve

During this reporting period, the experiments of plain pipe and that with sensor (using epoxy as an example) 1mm thick attachment on 6" pipe have been completed. The maximum axial loads were 1.13kN and 1.35kN for the plain pipe and pipe with 1mm sensor attached in the inner surface, respectively. The sensor's appearance after the pigging process is shown in Fig. 11. The sensor's outlook after the test shows that sensors with 1mm thickness could survive the motion of rubber disk, which means 1mm thickness is safe for epoxy-based sensors.



(a) Example sensor before test



(b) Example sensor after test

**Fig. 11.** Sensor's outlook

### 2.2.3 FEM Simulation Analysis for Sensor Size Optimization

#### 2.2.3.1 FEM Model Setup

Based on the Experimental parameters in last section, a two-dimensional slice Finite Element Model (FEM) was employed to analyze pigging process. The profile of the model is shown in Fig. 12 and Table 6 illustrates the detail parameters used in the FEM numerical analysis. The inner diameter of the steel pipe was assumed to be 154mm with a thickness of 7.1mm. Regular A36 steel was used as steel pipe material in the analysis. The disk on the cleaning pigs, also known as sealing disk, was assumed to have a thickness of 9.5mm and a diameter of 161 mm, which is 5% oversized when compared with the inner diameter of the pipe. The material of the sealing disk was assumed to be rubber. On the cleaning pigs, clamping plates are

usually made by steel to fix the sealing disks into proper space. In this analysis, as seen in Table 6, the thickness of the clamp plates was 6.4mm with an outer diameter of 76.2mm, which correspond with experimental arrangement. To reproduce the displacement of the Hydraulic loading Jig, the clamping plates were assigned a shift along the x-axis towards the right, forcing the sealing disk to move with them.

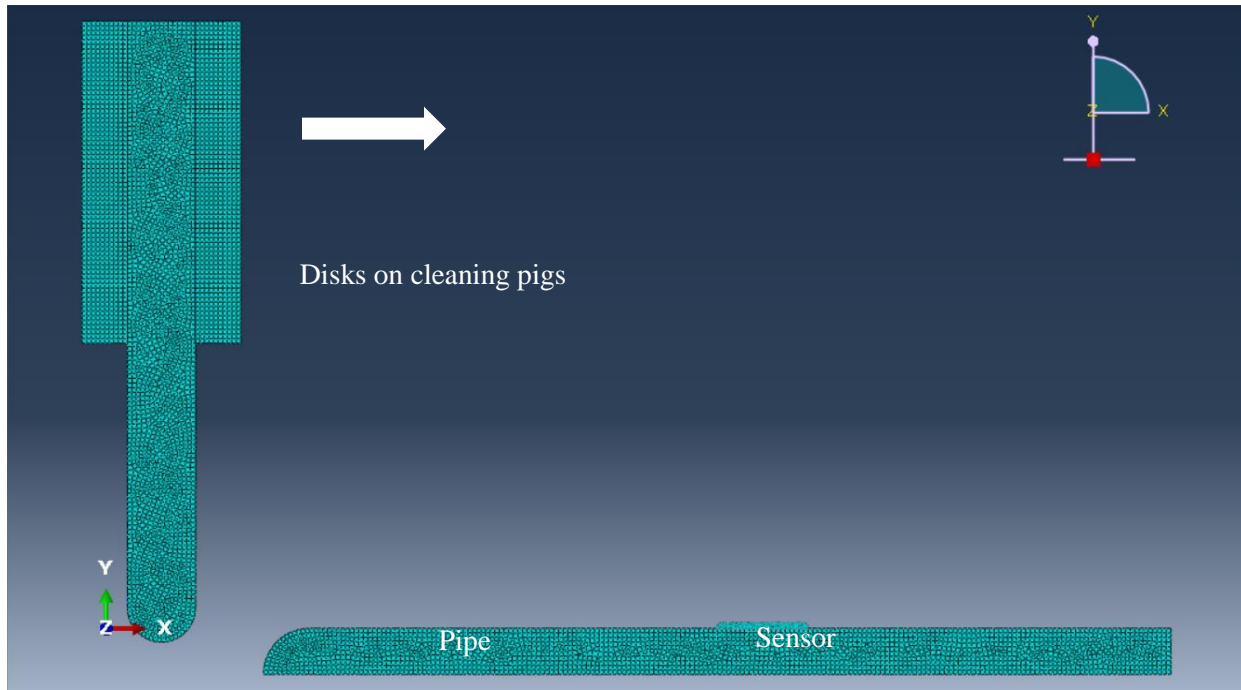


**Fig. 12.** FEM model sketch.

**Table 6.** FEM model dimension details.

Pipe inner diameter(mm)	Pipe thickness(mm)	Clamp plates thickness(mm)	Clamp plates outer diameter(mm)	Sealing disk thickness(mm)	Sealing disk outer diameter(mm)
154	7.1	6.35	200	9.5	161 (5% oversize)

In the FEMs, the material of the sealing disk, rubber, was considered as hyperelastic, which indicates high elasticity, ductility, and deformation restoring after unloading. Thus, the Mooney-Rivlin model, a hyperelastic material model, was used to simulate this material. In the Mooney-Rivlin model, the strain energy density,  $W$ , is a linear combination of two invariants of the left Cauchy-Green deformation tensor as shown in Equation 3. The detail material properties of the sealing disk used in the analysis are listed in Table 7.

$$W = C_1(I_1 - 3) + C_2(I_2 - 3) \quad (3)$$

in which,  $C_1$ ,  $C_2$  are the empirically determined material constants, and  $I_1, I_2$  are the first and second invariant of Cauchy-Green deformation tensor.

**Table 7.** Material properties of rubber (the sealing disk).

Density	Poisson's Ratio	Hardness (Shore A)	$C_{10}$	$C_{01}$
1350 kg/m <sup>3</sup>	0.35	85	1.926	0.963

Due to the fact that the simulation is performing simultaneously with the sensor development, at the time when the simulation was performed, the test results for the polymer selection were not available, in this report, for the sensor, we still assumed epoxy the polymer matrix to dope the chemical sensors. The material parameters of the epoxy (sensor) used in the analysis are listed in Table 8. If the sensor is ended up attaching to the pipe using epoxy, the analysis data will still be helpful for sensor analysis later. However, based on the most updated test results from this quarter, it can be seen that epoxy is not an appropriate polymer for writing the sensors in, so in next quarter, PMMA and other polymer (if available) will be analyzed. With the set-up model, the updates of these analysis should not be hard to perform.

**Table 8.** Material properties of epoxy (the sensor matrix).

Density(kg/m <sup>3</sup> )	Elastic (MPa)	Modulus Tensile (MPa)	Modulus Flexural (MPa)	Modulus Shear (MPa)	Modulus
1540	1000	10500	10000	1250	

### 2.2.3.2 Simulation Results

As the analysis in CAAP Project Quarterly Report #2, the simulation results can be analyzed using the deformation of the system. As illustrated from Fig. 13, the disk deforms when going through the pipe. Furthermore, a sensor attached on the inner surface of the pipe wall restricts the disk's deformation which leads to a higher stress in both rubber disk and the sensor.

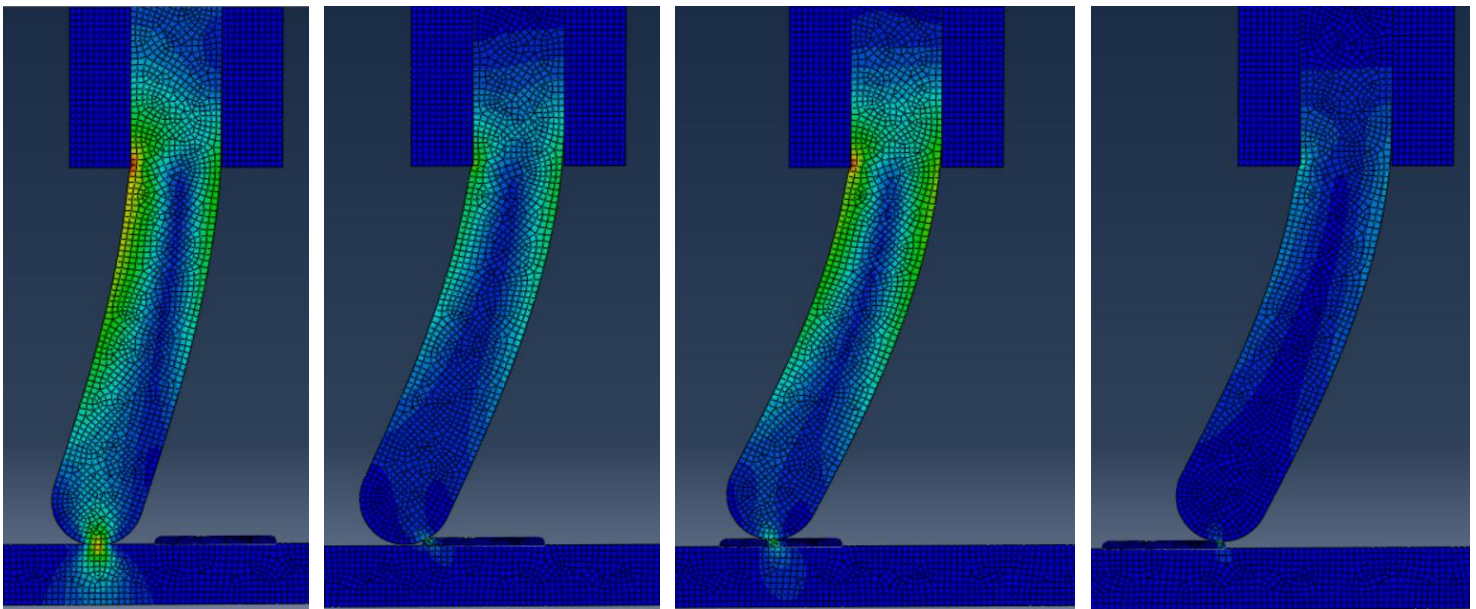


**Fig. 13.** FEM deformation results.

As also shown in Fig. 13, the process of the sealing disk passing the sensor can be divided into four stages: (1) start-up stage, (2) climbing stage, (3) scratch stage and (4) decline stage. In the first stage, the sealing disk began to come in contact with the sensor, the bending angle of the disk and contact stress began to increase. In the second stage, the bending angle and stress in the sensor increased sharply to a certain value, this is when maximum stress happened in the sensor. In the following stage, the sealing disk scratched the top surface of the sensor. The inner stress of the sensor remained relatively stable but less than the maximum stress experienced. In contrast, the stress of the sealing disk remained peaked during this progress. In the last stage, the sensor was unloaded due to the detachment from the sealing disk which reset to contact with the pipe. Compare with the experimental results, these 4 stages happen in the in-line procedure which

indicates the rubber plates passing through the inner wall of the pipe. In order to study the survivability of the sensor, the stress on the sensors are the main research subject rather than steel. To make a comparison of the experimental and simulation results, Mises Stress results from the simulation are shown in Fig. 14. It is shown that the maximum stress occurred on the 1mm thickness sensor is 3.02MPa according to the simulation.

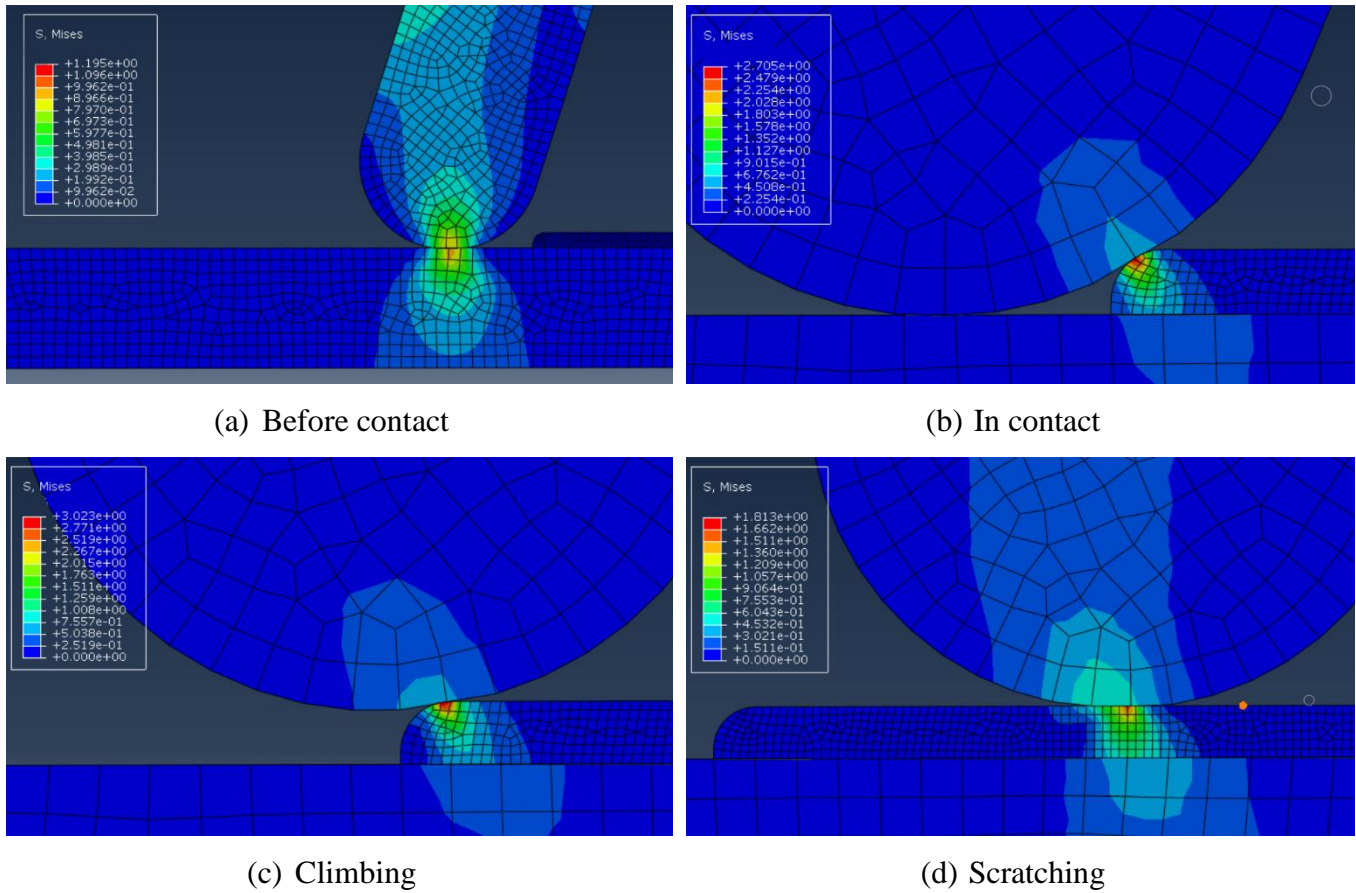


**Fig. 14.** Mises stress in the sensor from FEM analysis

### 2.2.3.3 Preliminary Analysis

From the experimental results, if the sensor is based on epoxy, it can survive a single pass of the rubber disk because of the small thickness. With a glance of the inner responses of the sensor from these two approaches, it can be seen that they have given the mechanical responses in different ways. For experiments, maximum axial load is the outcome, however, simulation gives the Mises stress which is the critical parameter of the study. To convert the axial load into stress in sensors, a conversion relationship should be established for verification purpose of the two approaches. Under the circumstance of the in-progress experiments and simulation, a preliminary conversion relationship has been chosen for the first-step validation. With the assumption that the contacting area of the disk and the pipe is a circular ring, the shear stress could be calculated by Equation (4) in which  $F$  is Axial load given by the experimental tests. However, for the contacting area, the axial distance is difficult to get compare to the computable perimeter of the inner pipe surface. In this situation, Equation (5) has been adopted to isolate the axial distance  $d$  as a coefficient of the calculation of  $A_r$ . In every analysis of the stress of a certain pipe,  $d$  should remain the same because of the same contacting area when the disk is going through. By the way of introducing the coefficient and the conversion of shear stress, validation of the simulation result with experiments is feasible

to reveal the survivability of the sensor under the PIG cleaning activities.

$$\tau_{sensor} = \frac{F}{A_r} \quad (4)$$

where,  $F$  is the axial load of experimental results, and  $A_r$  is the area of the contacting ring; and

$$A_r = l \times d \quad (5)$$

where,  $l$  is the perimeter of the inner pipe wall and  $d$  is the axial length.

In next quarter, we will compare the experimental results with the simulation using the relationships mentioned in Equations (3) and (4).

### **2.3 Student Mentoring**

During this quarter, four graduate students (Shuomang Shi, Ph. D. in Civil and Environmental Engineering at NDSU, Hafiz Usman Ahmed, Masters in Civil and Environmental Engineering at NDSU, and Jiapeng Lu, Ph.D. Student in chemistry at NDSU, Baiyu Jiang, Ph.D. in Civil Engineering at Rutgers University) and two undergraduate research assistants (Gina Blazanin and Alex Glowacki) were hired to work on this project. The four graduate students will work on this project from Quarter 5 to Quarter 6 of this project. The two undergraduate students were hired from October 2019 to December 2019. New undergraduate research assistants will be hired in January 2020 for the next quarter of this project.

### **3. Future work**

In the 5<sup>th</sup> quarter, there will be three objectives:

- 1) Task 2.1: Select and test some other porous polymeric materials for the sensor matrix for  $\text{HCO}_3^-/\text{CO}_3^{2-}$ ,  $\text{S}^{2-}$ ,  $\text{Fe}^{3+}$ , and  $\text{H}^+/\text{pH}$ ;
- 2) Task 2.2: Conduct and complete the experiment tests along with relevant FEM simulations for survivability of sensors, and validate the results from these two approaches to reliable models for sensor's survivability under PIG activities;
- 3) Task 2.2: Conduct experimental research on the survivability under normal serving condition, including oil/gas or water environment;
- 4) Task 2.3: Start optimizing the  $\text{Fe}^{2+}$  in PMMA;
- 5) Task 3: *Select the corrosion model to be used for corrosion prediction.*